Single Nanoparticle Spectroscopy: An Analysis of Sample Preparation and Microscopy Techniques

Undergraduate Researcher
W. Paige Hall, University of Notre Dame

Faculty Mentors
Greg Hartland
Department of Chemistry, University of Notre Dame

Richard Van Duyne
Department of Chemistry, Northwestern University

Graduate Mentor
Hristina Petrova
Department of Chemistry, University of Notre Dame

Abstract

This paper explores the various approaches to time-resolved single nanoparticle spectroscopy. Due to the novelty of these types of experiments, several difficulties arise in creating a feasible physical setup capable of imaging single nanoparticles less than 100 nm in size. The various difficulties in setup and their attempted resolutions will be discussed, placing particular emphasis on gold and silver nanoparticle synthesis, sample preparation, and details of spectroscopic setup and methods. It will be shown that total internal reflection microscopy in conjunction with careful sample preparation is a promising step toward investigating the material properties of single nanoparticles.

Introduction

Striking advances have been made in the field of nanotechnology in the last several years, particularly in the areas of nanoparticle synthesis and spectroscopic analysis. Research in these areas is driven by the desire to manipulate the unique properties of nanoscale materials for technological and medical applications. The unique optical, electromagnetic, and thermodynamic properties of metal nanoparticles have made them useful in a variety of applications including biomedical sensors,[1] probing devices, drug administration, optical data storage,[2] and electronic and semiconductor devices. However, for metal nanoparticles to be applied effectively to technological advances, something must be known of their material properties, which can vary significantly from that of their bulk counterparts. As one can imagine, the size scale of nanoparticles can make such observations of material properties difficult.

A useful way to investigate these properties has been to use time-resolved spectroscopy.[3–7] Typically, this method involves exciting a sample with a high-energy pump laser pulse, then "looking" at the sample response with a delayed-probe laser pulse. The excitation process involves exciting electrons to higher energy levels, causing a rapid heating of the electron distribution. The hot electron distribution then cools down by sharing its heat with the phonon modes through electron-phonon coupling. Finally, the excess energy is dissipated through phonon-phonon coupling with the local environment. The "looking" process most often involves monitoring changes in the absorption spectrum of the sample as these excitation and relaxation processes occur. Fortunately, the absorption spectrum is known as a function of nanoparticle size, shape, temperature, and composition. This means that changes in sample morphology in response to laser excitation, such as melting and fragmentation, create changes in the absorption spectrum that can easily be understood.

While time-resolved spectroscopy is a useful way to study samples with a meaningful optical density, such as solutions or films, the study of single nanoparticles is somewhat more challenging. A primary obstacle is that single nanoparticles show negligible absorption. This problem can be circumvented by focusing instead on particle scattering. Although particles of less than 10 nm diameter do not significantly scatter light, scattering is very pronounced for nanoparticles in the 30–100 nm diameter range and thus is a useful alternative to traditional absorption measurements.[8]

To observe the scattering of single particles, it is necessary to use a setup in which the background light can be totally blocked. This is commonly accomplished using either dark-field or total internal reflection microscopy. Dark-field microscopy in transmission has the advantage of employing a traditional microscope setup, with one exception: a dark-field condenser is used, which focuses light onto the sample at a large angle. The transmitted light does not enter the objective, and thus the light seen through the microscope is only that which has been scattered by the sample. With total internal reflection microscopy, the incident light is reflected rather than blocked. As the name suggests, the setup requires the use of a prism that completely reflects all incident light due to differences in the refractive index of the prism and the substrate surface. As with the dark-field setup, only light scattered by the particles propagates out of the evanescent wave and enters the objective.

This paper will discuss the various advantages and disadvantages of each setup as it applies to the imaging of single nanoparticles. A primary obstacle in these experiments is sample preparation. Obviously, to gain an appropriate understanding of single nanoparticle behavior, the samples must be prepared with enough space between particles to eliminate coupling effects. Ideally, each particle should also be far enough from its neighbor so that only one particle at a time is

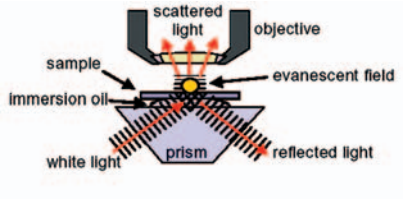

Figure 1: Diagram of total internal reflection setup. The setup used in this study only differed in that the sample and objective were flipped 180 degrees, so that the incident light was directed from above.

illuminated by the pump and probe laser pulses. In addition to sample preparation, this paper will discuss various nanoparticle synthesis methods as well as the observation of single-particle scattering spectra using a total internal reflection microscope setup.

Background

Much research has been done on the electron dynamics of nanoparticles using transient absorption spectroscopy. Among other things, research in this area has revealed changes in electronic and lattice vibrational properties[9] as well as morphological changes upon laser-induced excitation. Hodak et al described the absorption spectra of Au-Ag core-shell nanospheres, using postexcitational changes in the spectra and transmission electron microscopy (TEM) to demonstrate melting and interdiffusion of the two metals.[10] Surface melting was shown to occur at temperatures much lower than that of the bulk metal. Hartland et al observed changes in the symmetric breathing mode of gold spheres upon high lattice heating. The period of the breathing mode was shown to increase with increasing pump laser power up to the melting point of gold, though temperatures higher than the melting point were not achieved.[11] The vibrational modes of gold nanorods were investigated by Hu et al, revealing that the extensional and breathing modes of the rod dominate vibrational excitation.[12] Most recently, Eah et al demonstrated correlations between morphology and transient absorption in gold nanocrystal monolayers and an e-ph coupling constant in agreement with that of bulk films.[9]

While the preceding experiments have revealed important information about the dynamics of bulk samples, the properties of individual particles are still widely unknown. In addition, because coupling effects contribute significantly to the physical, chemical, and optical properties of particles, the behavior of isolated nanoparticles could deviate significantly from that of films. Significant progress has been made by McFarland et al toward an experimental setup capable of elucidating the properties of single particles.[13] Using dark-field microscopy, the authors were able to observe the plasmon resonance of single Ag nanoparticles and demonstrated a real-time response to small-molecule adsorbates. Sönnichsen et al used a total internal reflection setup to measure the scattering spectra of single particles fabricated by electron beam lithography.[14] Time-resolved scattering spectroscopy of individual particles was accomplished by Matsuo and Sasaki.[15]

This research project aims to expand on previous single nanoparticle studies by investigating the material properties of metal nanoparticles. This is accomplished by using total internal reflection microscopy coupled with a pump-probe laser setup as described in the next section.

Approach

As discussed previously, the problem arising from the negligible absorption of single nanoparticles can be circumvented by focusing instead on particle scattering, which can be observed with dark-field and total internal reflection microscopy. Because our ultimate goal is to conduct time-resolved spectroscopy experiments, geometry is a major factor in choosing an appropriate setup. In this regard, total internal reflection microscopy confers a great advantage. Since the sample is illuminated at an angle, a pump-probe laser

system can easily be set up without compromising the microscope arrangement.

The pump-probe system used here utilizes a Ti:Sapphire laser at 780 nm. The emitted light beam is split using a beam splitter into a "pump" beam and a "probe" beam. The wavelength of the probe beam is doubled using a doubling crystal to approximately 400 nm. The two beams are then routed using mirrors and lenses until they are once again concurrent and pass through the prism to illuminate the sample at approximately a 45-degree angle (Figure 1). The sample itself was prepared by drop-coating either the prism surface or a standard coverslip with aqueous gold or silver solution and allowing it to air dry. A drop of index matching fluid was placed on the prism surface, and the coverslip was adhered at the corners using clear nail enamel.

Early in the experimental process, it was discovered that impurities or scratches on the prism surface led to misleading light scattering. Therefore, sample preparation became a major issue, and both coverslip and prism were cleaned thoroughly by first sonicating in one molar hydrochloric acid, followed by sonication in 95 percent ethanol, and finally a careful wipedown using methanol and a high-quality lens wipe. Particles in the sample also had to be evenly distributed and ideally spaced several to tens of micrometers apart. To achieve this, we experimented with various dilutions of the sample solution and used both drop-coating and spin-coating techniques.

Because of their unique spectral properties, gold and silver nanoparticles of various shapes and sizes were investigated. Two silver solutions were synthesized — one using standard citrate synthesis, and another using sodium borohydride reduction, which yielded slightly larger particles. Both syntheses produce extremely polydisperse particles. Gold spheres of 50 nm diameter were synthesized by radiation chemistry in a method detailed by Henglein et al.[16] Gold rods of 90 nm length and 11 nm radius were synthesized using the seed-mediated growth technique developed by C. Murphy.[17] All samples were in aqueous solution and used without any further modification.

Results

While single-particle plasmon spectra were not taken for the synthesized nanoparticles, a plasmon spectrum was obtained for each synthesis in solution. The sodium borohydride synthesis of silver yielded a clear yellow solution with a peak extinction wavelength (λ_{max}) near 410 nm. The citrate synthesis of silver produced a milky greenish-brown solution. The plasmon spectrum of this solution was extremely broad, and no clear λ_{max} could be determined. This is most likely due to both the cloudiness of the solution and the polydispersity of the silver particles. The synthesis of 50 nm gold spheres produced an iridescent (due to scattering) pink solution with a λ_{max} near 525 nm. Finally, the gold rod synthesis yielded a clear pink solution with a λ_{max} near 530 nm.

Once it was discovered that samples prepared on the prism were particularly prone to contamination, a dark-field setup was used in conjunction with atomic force microscopy (AFM) study to improve preparation techniques. Initially, samples were prepared by drop-coating the substrate, either the prism surface or a coverslip, and allowing it to air dry. Samples prepared using this method showed vivid scattering. An advantage to the polydispersity of the silver samples was the variety of colors scattered by the

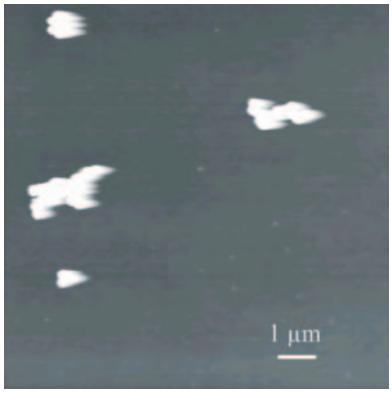

Figure 2: Drop-coated sample of 50 nm gold spheres. Note that the particles do not disperse but aggregate together in clusters. Streaking in image is an AFM artifact.

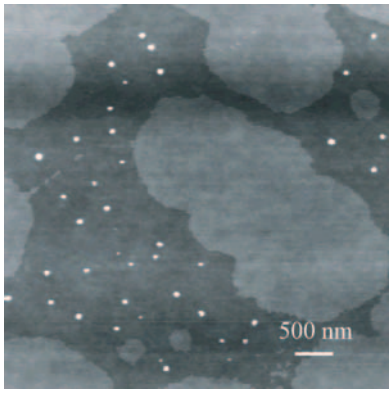

Figure 3: A spin-coated sample of silver particles synthesized using $NaBH_4$ reduction. This image reveals that spin-coating produces evenly spaced, isolated particles. The splotches here are due to the sample solution and did not interfere with dark-field scattering.

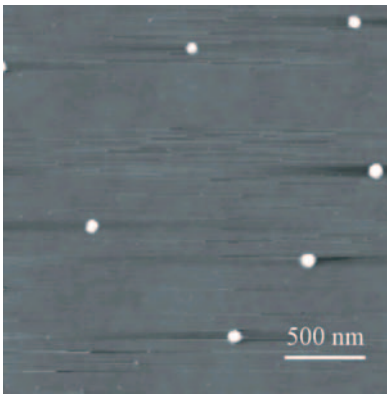

Figure 4: Gold nanorods of 90 nm length and 11 nm radius. Linescan analysis also revealed the presence of oblate particles. Particles are isolated and evenly spaced.

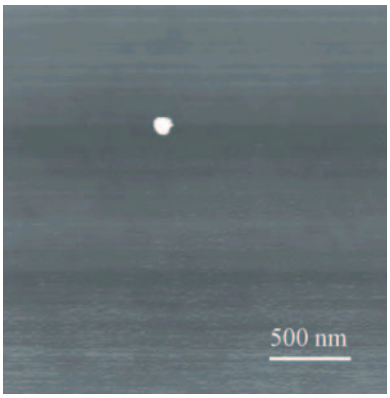

Figure 5: Gold spheres of 50 nm diameter. This sample contained only isolated and widely-spaced particles, ideal for single-particle spectroscopy.

particles. Previous work has shown that triangular particles scatter red light, polygonal particles scatter green, and spheres scatter blue.[18] While drop-coating produced samples with a large number of particles ideal for viewing scattering, AFM images revealed that the particles aggregated into numerous large clusters (Figure 2). Simply diluting the sample proved ineffective in eliminating the particle clusters.

The next technique adopted involved spin-coating the samples on a spin-coater designed for wafer fabrication. This method was effective in preventing the aggregation of particles in both silver and gold solutions. Various dilutions were prepared and spin-coated on a round 15 mm glass coverslip flamed with a gas torch to produce a hydrophilic surface. Figure 3 shows an AFM image of a sample coated with a 1/100 dilution of silver prepared using sodium borohydride reduction. The scale reveals that the particles are spaced approximately 500 nm apart, too close for effective single-particle spectroscopy. However, it is important to note that the particles are evenly spaced, suggesting that further dilution will be sufficient to isolate the particles. A curious side effect of the sodium borohydride preparation is the appearance of solvent splotches on the sample. This did not interfere with scattering as observed using dark-field microscopy.

Figure 4 shows an AFM image of a spin-coated sample of gold nanorods of 90 nm length and 11 nm radius. Again, the particles are evenly spaced though not dispersed enough for the AFM to focus on a single particle. As with the previous sample, this can be remedied by further diluting the solution. Linescan analysis reveals that the particles are somewhat polydisperse, with spheres as well as the expected rods appearing in solution. Finally, a spin-coated sample of concentrated 50 nm diameter gold spheres produced evenly spaced, isolated particles at distances conducive to single-particle spectroscopy (Figure 5). The particle shown is in an area of approximately 6.25 μm^2, and imaging of adjacent areas revealed no other nearby particles.

Most important, using total internal reflection microscopy, we succeeded in gathering single-particle scattering spectra of a silver sample prepared using $NaBH_4$ reduction. The microscope used in these experiments is connected to a spectrograph that is coupled to a charged coupled device (CCD) to enable spectral imaging. By replacing the spectrograph, diffraction grating with mirror particles could be viewed as a function of their scattering intensity. This function was particularly valuable in correlating the camera image from the microscope with the image detected by the spectrograph. Several trials revealed that the two fields of view were in agreement. As a point of reference, the scattering image of a single silver nanoparticle adjacent to a cluster of particles was taken with the mirror in place. The mirror was then replaced with a diffraction grating at 500 nm wavelength in order to record the scattering spectra. It was apparent in this spectra that two distinct objects are being imaged corresponding to the single nanoparticle and the adjacent cluster. A cross-section of the single-particle spectrum revealed a peak at 660 nm (Figure 6), while a cross-section of the cluster revealed a slightly narrower spectrum with a peak near 600 nm (Figure 7). Both of these values are within the range of expected scattering spectra of nonspherical silver particles.

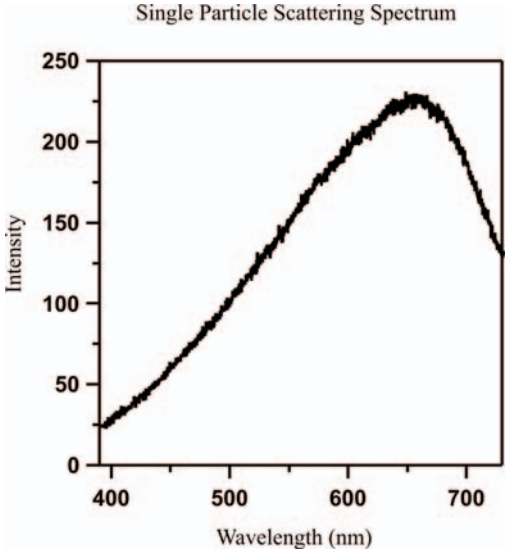

Figure 6: Cross-section of the scattering of a single silver nanoparticle.

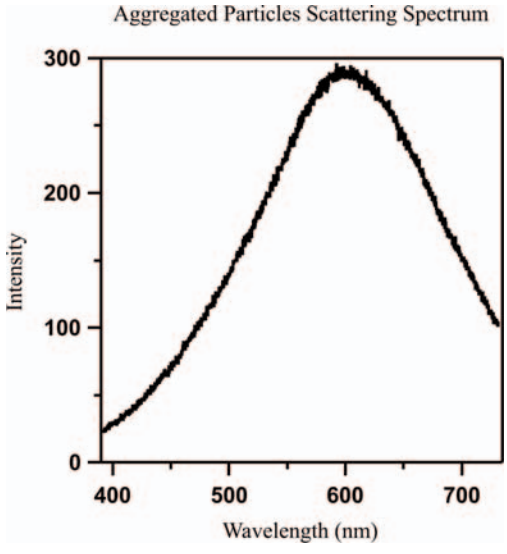

Figure 7: Cross-section of the scattering of what appeared to be an aggregate of several silver nanoparticles.

Discussion

The issues with sample preparation presented here are perennial problems in single-particle spectroscopy. Other groups have created viable samples using nanosphere lithography[13] or electron beam lithography.[14] However, AFM images of our samples reveal that appropriate particle spacing can be achieved by merely spin-coating the substrate with an aqueous sample solution. Taking into account the cross-sectional area of the light source and interparticle coupling, spacing of 10 μm is a general guideline for the minimum interparticle distance necessary for single-particle spectroscopy. The AFM images presented here reveal that, using an appropriate sample dilution, this criteria can be met using the spin-coating technique.

There are two important things to note regarding the scattering spectra presented here: the λ_{max} of each spectra lies within the expected range of λ_{max} for nonspherical silver particles, and the spectra exhibit a very broad full width at half maximum (FWHM). The former observation is promising in that it suggests the total internal reflection setup used here is successful in gathering single-particle scattering spectra. The position of λ_{max} is highly dependent on particle shape and can range from around 400 nm for spherical particles to near 800 nm for sharp-edged triangles. While solitary particles generally exhibit a blue shift relative to aggregate particles, the red shift in the single-particle spectrum relative to the cluster spectrum can be interpreted to mean that the particle has a sharper, less rounded shape, though the precise particle from which the spectrum was taken could not be characterized using AFM. However, the wide FWHM of the spectrum is characteristic of a polydisperse sample, suggesting that the spectrum gathered was not that of a single nanoparticle but rather a collection of nanoparticles. It is known that the $NaBH_4$ synthesis produces silver particles of a variety of shapes and sizes, and this was confirmed by AFM linescan analysis. Therefore, if the scattering spectrum presented here was recorded from multiple rather than single nanoparticles, a wide FWHM and relative red shift is to be expected.

Another explanation for the wide FWHM observed for both spectra is the presence of background noise. Ambient light as well as residue from the sample solution can create background noise and interfere with the particle's scattering spectrum. In addition, larger particles are known to produce spectra with larger FWHM.[14] AFM linescan measurements revealed that the $NaBH_4$ reduction produced silver particles with an average height of 10 nm and width of 128 nm, which are likely to produce a broad spectrum as shown here. These problems can be alleviated in future studies by subtracting background noise from the particle spectra and experimenting with more monodisperse synthesis techniques.

Conclusions

The most important conclusions of this research involve the issues of sample preparation and the collection of single-particle scattering spectra. It was shown that spin-coating a substrate with aqueous sample solutions can result in samples with isolated and evenly distributed particles ideal for use in single-particle spectroscopy. This method is not only effective in producing appropriate particle geography but also has a vast cost advantage over other preparation methods such as electron beam lithography and nanosphere lithography. The preparation using aqueous sample solution and spin-coating offers the ability for more labs to study nanoparticle behavior with a low-cost, time-efficient technique.

In addition, the total internal reflection microscopy setup Sönnichsen described was reproduced, enabling the observation of particle scattering. The scattering of presumed single nanoparticles was observed using both a camera and CCD apparatus, and the scattering spectrum of both single and multiple particles was gathered. These are not novel accomplishments, but successful gathering of a single-particle scattering spectrum is an important step toward the ultimate goal of conducting time-resolved spectroscopy on single particles. Currently, our research is aimed at fine-tuning the pump-probe laser setup in order to observe the dynamics of particle scattering. Once accomplished, time-resolved spectroscopy will yield valuable insights into the electron dynamics of single nanoparticles and contribute to the eventual application of single nanoparticles in many medical and technological devices.

References

(1) Haes, A. J.; Hall, W. P.; Chang, L., et al. *Nano Lett.* **2004**, *4*, 1029–1034.

(2) Ditlbacher, H.; Krenn, J. R.; Lamprecht, B., et al. *Opt. Lett.* **2000**, *25*, 563.

(3) Zhang, J. Z. *Acc. Chem. Res.* **1997**, *30*, 423.

(4) Link, S.; El-Sayed, M. A. *J. Phys. Chem.* B **1999**, *103*, 8410.

(5) El-Sayed, M. A. *Acc. Chem. Res.* **2001**, *34*, 257.

(6) Hodak, J. H.; Henglein, A.; Hartland, G. V. *J. Phys. Chem. B* **2000**, *104*, 9954.

(7) Voisin, C.; Del Fatti, N.; Christofilos, D., et al. *J. Phys. Chem. B* **2001**, *105*, 2264.

(8) Sönnichsen, Carsten. *Plasmons in Metal Nanostructures.* Dissertation at Ludwig-Maximilians-University of Munich.

(9) Eah, S.; Heinrich, M. J.; Scherer, N. F., et al. *Chem. Phys. Lett.* **2004**, *386*, 390–395.

(10) Hodak, J. H.; Henglein, A.; Giersig, M., et al. *J. Phys. Chem. B* **2000**, *104*, 11708

(11) Hartland, G. V.; Hu, M.; Sader, J. E. *J. Phys. Chem. B* **2003**, *107*, 7472–7478.

(12) Hu, M.; Wang, X.; Hartland, G. V., et al. *J. Am. Chem. Soc.* **2003**, *125*, 14925–14933.

(13) McFarland, A.; Van Duyne, R. P. *Nano Lett.* **2003**, *3*, 1057–1062.

(14) Sönnichsen, C.; Geier, S.; Hecker, N. E., et al. *Appl. Phys. Lett.* **2000**, *77*, 2949–2951.

(15) Matsuo, Y.; Sasaki, K. *Jpn. J. Appl. Phys.* **2001**, *40*, 6143–6147.

(16) Henglein, A.; Meisel, D. *Langmuir* **1998**, *14*, 7392–7396.

(17) Jana, N. R.; Gearheart, L.; Murphy, C. J. *J. Phys. Chem. B* **2001**, *105*, 4065–4067.

(18) Mock, J. J.; Barbic, M.; Smith, D. R., et al. *J. Chem. Phys.* **2002**, *116*, 6755–6759.